Vision Res. Vol. 16, pp. 1407 to 1418. Pergamon Press 1976. Printed in Great Britain.

ADAPTATION TO A SPATIAL IMPULSE: IMPLICATIONS FOR FOURIER TRANSFORM MODELS OF VISUAL PROCESSING

GORDON E. LEGGE
Harvard University, Cambridge, MA 02138, U.S.A.

(*Received* 15 *October* 1975; *in revised form* 30 *March* 1976)

Abstract—Spatial frequency adaptation was analyzed in terms of three representative models of the Fourier transform theory of visual processing. Each model predicted that subjects who exhibited normal sine-wave grating adaptation should show substantial adaptation over a wide range of spatial frequencies following exposure to a narrow bar of high luminance (one-dimensional spatial impulse). In the experiments, two highly practiced subjects who showed normal sine-wave adaptation, showed little adaptation to a 140 cd/m^2 bar subtending 0.6′, superimposed on a background of 4.63 cd/m^2 subtending 1.75°. Two control experiments with a third subject indicated that neither a photoreceptor nonlinearity nor a power function transformation of the luminance distribution could account for the discrepancy. The lack of adaptation to the spatial impulse suggests that present Fourier transform models which postulate phase-independent frequency channels in the visual system are inadequate for the description of the visual response to suprathreshold aperiodic stimuli. A receptive field model of spatial frequency processing and phase encoding is suggested to account for the results.

Key Words—spatial frequency adaptation; Fourier transform; sine-wave grating; spatial impulses; receptive field; phase.

INTRODUCTION

Campbell and Robson (1968) proposed that the human visual system processes spatially varying luminance distributions by means of a set of independent spatial frequency channels. Each of the channels possesses its own spatial frequency sensitivity characteristic, often termed its modulation transfer function or MTF. The overall spatial frequency response of the visual system is assumed to be the envelope of these. Their proposal was based on the evidence that, at pattern threshold, the relative visibility of periodically varying luminance distributions is determined by the relative magnitudes of their spectral components. Subsequently, their proposal has stimulated a vast amount of important research and has received support from a variety of psychophysical and physiological experiments. Notable among these are the observations of critical band masking in vision (Stromeyer and Julesz, 1972), the apparent size shift after-effect (Blakemore and Sutton, 1969), and the spatial frequency adaptation phenomenon (Pantle and Sekuler, 1968; Blakemore and Campbell, 1969).

The spatial frequency adaptation phenomenon, first demonstrated by Pantle and Sekuler (1968), and then extensively studied by Blakemore and Campbell (1969), is the increase in pattern threshold for the detection of a sine-wave luminance distribution following exposure to a similar sine-wave luminance distribution of high contrast. It is observed that the threshold elevation is constrained to a limited band of frequencies surrounding the adapting frequency. A behavioural measure of the adaptation phenomenon, first introduced by Blakemore and Campbell (1969), is the relative threshold elevation $R(f)$, defined as:

$$R(f) \equiv \frac{T_a(f) - T_b(f)}{T_b(f)} = \frac{T_a(f)}{T_b(f)} - 1, \qquad (1)$$

where $T_a(f)$ is the nominal contrast at threshold of a sine-wave target of frequency f after adaptation, and $T_b(f)$ is the nominal contrast at threshold of a sine-wave target of the same frequency before adaptation. For a one-dimensional sine-wave luminance distribution of amplitude a, frequency f_0, and mean luminance L_0, described by

$$L(x) = L_0 + a\sin(2\pi f_0 x)$$

the nominal contrast is defined to be:

$$c_{f_0} \equiv a/L_0.$$

Under adaptation to high contrast sine-wave gratings, Blakemore and Campbell (1969) have observed relative threshold elevations of 4 or more, i.e. increases in the nominal contrast at threshold by factors of 5 or more.

The existence of spatial frequency adaptation and its limited band-pass characteristic is often interpreted as explicit evidence for a set of independent spatial frequency channels in the visual system. On the basis of their work, Blakemore and Campbell (1969) extended the proposal of Campbell and Robson (1968) to postulate a Fourier decomposition model for visual processing. They proposed that suprathreshold luminance distributions are decomposed by the visual system into their Fourier components and that these are passed along independent neural channels. The set of channels may be compared to a set of independent,

parallel, band-pass filters, each followed by its own detector. After prolonged stimulation, these channels adapt and thereby behaviourally manifest themselves and their frequency bandwidth through decreased sensitivity.

At present, the Fourier decomposition model is supported by many suggestive, but strictly qualitative, observations of spatial frequency selective phenomena (Campbell, 1974). If the Fourier transform theory is to be useful in describing the means by which visual information is processed, it should have predictive power when applied to the analysis of visual response to arbitrary stimulus patterns, in particular, aperiodic patterns. The analyses and experiments reported here will show that the Fourier transform theory, when given predictive power by a representative set of empirically based phase-independent models, makes rather dramatic predictions which are not confirmed, concerning the processing of a bright, narrow, luminance bar, or spatial impulse. The three models are formulated in terms of assumptions necessary to any Fourier decomposition model, together with empirical specifications of channel MTF and stimulus/response functions which circumscribe the variety of findings in the literature. As such, these models are broadly representative, and tests of their validity will be crucial to an evaluation of the simple Fourier transform theory of visual processing. An alternative linear model, that includes a particular mechanism of phase encoding, will be suggested to account for the empirical results to be reported.

FOURIER TRANSFORM MODELS OF SPATIAL FREQUENCY ADAPTATION

In this section, three quantitative models are developed, each compatible with a Fourier decomposition theory, which make predictions of the adapting effect of any arbitrary luminance distribution. These three models have been chosen as representative extensions of the qualitative models presently extant in the literature. They are all based upon the modulation transfer function approach, first used in linear optics (Linfoot, 1964) and as such, they are phase-independent. The question of phase-encoding will be taken up in the Discussion. Empirical tests of the three Fourier transform models will now be discussed.

Before formulating the three models, it is necessary to define spatial, spectral, and nominal contrast.

The spatial contrast function, $c(x)$, representing a luminance distribution, is given by:

$$c(x) \equiv \frac{L(x)}{L_0} \tag{2}$$

where x is the spatial coordinate (in this paper, in degrees of visual angle), $L(x)$ is the luminance distribution (in this paper, cd/m^2), and L_0 is the mean luminance of the distribution.

The spectral contrast function, $C(f)$, is the Fourier transform of the spatial contrast function $c(x)$:

$$C(f) \equiv \frac{L(f)}{L_0} \tag{3}$$

where $L(f)$ is the Fourier transform of $L(x)$:

$$L(f) = \int_{-\infty}^{\infty} L(x)\, e^{-2\pi i x f}\, dx.$$

The nominal contrast of a sinusoidal luminance distribution is the ratio of the amplitude, a, of the sinusoidal modulation to the mean luminance, L_0:

$$c_{f_0} \equiv \frac{a}{L_0} \tag{4}$$

where f_0 is the nominal frequency of the sinusoidal modulation. This is the definition of contrast most widely used in the spatial frequency literature.

Any quantitative Fourier model of spatial frequency adaptation must specify the following: (1) the channel MTF—i.e. the spatial frequency sensitivity function of the adapting channel; (2) the stimulus/response characteristics of the channels; for instance, given the MTF of the channel, is its response proportional to the integrated power spectrum, to the magnitude spectrum, or some other property of the filtered stimulus? (3) How is the response of the channel related to its adaptation as measured by the relative threshold elevation function $R(f)$?

These three questions are taken up in the following three subsections.

MTF of the spatial frequency channels

If the visual system performs a strict Fourier analysis, the band-width of its channels will be infinitely narrow. Their response will be in proportion to the magnitude (or energy density) of the stimulus spectrum at the channel frequency. However, if spatial frequency adaptation is presumed to be a consequence of neural activity in spatial frequency channels, then the frequency selectivity of the adaptation effect suggests that the channels themselves have a rather broad, band-pass characteristic. It is empirically observed that pattern threshold is elevated at frequencies well beyond the spectral breadth of the adapting sinusoidal stimuli.

The band-width of spatial frequency selectivity found in adaptation studies (Blakemore and Campbell, 1969) has been largely confirmed in studies of critical band masking (Stromeyer and Julesz, 1972), studies with frequency-modulated gratings (Stromeyer and Klein, 1975), and studies of line detection and probability summation (King-Smith and Kulikowski, 1975). However, studies of the detectability of complex periodic stimuli consisting of two sinusoidal components (Sachs, Nachmias and Robson, 1971; Quick and Reichert, 1975), have suggested much narrower frequency selectivity. The various possibilities can be bracketed by the following two cases, to be incorporated into the models below.

(a) The channels are infinitely narrow—the channel designated f_0 responds in proportion to some function of the stimulus Fourier transform at frequency f_0.

(b) The channel's MTF is represented by the following function:

$$\mathrm{MTF}_{f_0}(f) = \exp\left[-\left(\frac{4|f - f_0|}{f + f_0}\right)\right]. \tag{5}$$

This is a function of width about 1.5 octaves between (1/e) points, peaking at frequency f_0. It is a slightly narrower function than the MTF proposed by Blakemore and Campbell[1] (1969) and represents a conservative approxi-

[1] Blakemore and Campbell (1969) proposed an MTF represented by the function

$$(e^{-f^2} - e^{-4f^2})^2.$$

mation to it. The exact shape of the proposed MTF will be unimportant to the results below.[2]

Stimulus/response characteristic

It will be assumed that any given spatial frequency channel responds in proportion to the integral over frequency of some functional of the filtered stimulus spectrum. In mathematical notation, if r_{f_0} is the response of a channel maximally sensitive to frequency f_0, it is assumed that:

$$r_{f_0} \propto \int_0^\infty F[C(f)\mathrm{MTF}_{f_0}(f)]\,df \tag{6}$$

where[3] $C(f)$ is the spectral contrast function of the stimulus, F is some function, as yet unspecified, and $\mathrm{MTF}_{f_0}(f)$ is the MTF of the channel maximally sensitive at frequency f_0. A stimulus/response of this form occurs in an electric circuit in which a response device, such as a voltmeter, is preceded by a linear filter. r_{f_0} corresponds to the reading of the voltmeter, the functional F determines whether the meter's response is proportional to the RMS level or some other property of the input waveform, $c(f)$ is the spectral representation of the input waveform and $\mathrm{MTF}_{f_0}(f)$ corresponds to the band-pass filter characteristic with peak sensitivity at frequency f_0. The form of the function F has been considered in connection with the dependence of the system MTF upon the number of cycles of a sine-wave grating (Hoekstra, van der Goot, van den Brink and Bilsen, 1974; Savoy and McCann, 1975). For present purposes, the following two simple forms of the function F will be proposed as representative.

(a) First:

$$F[C(f)\mathrm{MTF}_{f_0}(f)] = C(f)\mathrm{MTF}_{f_0}(f). \tag{7}$$

Here, the spatial frequency channel responses will be sensitive to the filtered spectral contrast function of the stimulus luminance distribution.[4]

(b) Second:

$$F[C(f)\mathrm{MTF}_{f_0}(f)] = [C(f)\mathrm{MTF}_{f_0}(f)]^2. \tag{8}$$

Here, the spatial frequency channel response is sensitive to the "power spectrum" or spectral "energy density" of the filtered stimulus distribution.

These two proposed forms will be incorporated into the models presented below.

Relation between channel response and relative threshold elevation

The behavioural variable that will be used as a measure of spatial frequency adaptation is the relative threshold elevation $R(f)$, defined in equation (1).

It is an empirical result (Blakemore and Campbell, 1969, Fig. 4; Tolhurst, 1972, Figs. 1–5), that relative threshold elevation rises very slowly with the nominal contrast c_{f_0} of an adapting sinusoidal grating. In fact, it is clear from their data that the relation between the maximum value of $R(f)$ and c_{f_0} is well approximated by a power functon of the form $R(f) = k(c_{f_0})^n$, up to some saturating level, whereupon the adaptation increases no further. An estimated lower bound for the power function exponent as derived from the data of Blakemore and Campbell (1969) and Tolhurst (1972), is a value of 0.20. This value will be used below. It represents a conservative estimate, and any larger exponent would lead to a more striking rejection of the models to be proposed. Thus, the relation between the relative threshold elevation, $R(f_0)$, of a channel with peak frequency sensitivity at f_0, and the nominal contrast c_{f_0} of an adapting grating of nominal frequency f_0 is assumed to be:

$$R(f_0) = k(c_{f_0})^{0.20} \tag{9}$$

where k is a constant of proportionality.

Three Fourier transform adaptation models

In the previous three subsections, two representative channel MTFs, two representative stimulus/response functions, and a relation between the relative threshold elevation and the nominal contrast of a sine-wave grating stimulus, have been proposed. By crossing the two candidate MTFs with the two stimulus/response functions, four hypothetical channel response functionals are obtained. Each of these can be related to the relative threshold elevation function by means of equation (9). Two of these hypothetical response functionals yield identical predictions and therefore can be included in a single model.

Model 1. In Model 1, it will be assumed that the response of a spatial frequency channel of peak sensitivity at frequency f_0 is proportional to the integral over frequency of the spectral contrast function of the stimulus, weighted by the channel's broad-band MTF:

$$r_{f_0}^{(1)} \propto \int_0^\infty C(f)\exp\left[\frac{-4|f-f_0|}{f+f_0}\right]df \tag{10}$$

where $r_{f_0}^{(1)}$ is the hypothetical response of a spatial frequency channel at f_0, under Model 1. Under sine-wave grating stimulation, $C(f)$ is proportional to c_{f_0}, the nominal contrast of the grating. In equation (9), it has been assumed that the relative threshold elevation is related to the nominal contrast by a power function with an exponent of 0.20. Thus, the relative threshold elevation of a channel will be related to its response by a power function of the same exponent. From equations (9) and (10):

$$R_{f_0}^{(1)} = k_1(r_{f_0}^{(1)})^{0.20} = k_1\left[\int_0^\infty C(f) \times \exp\left[\frac{-4|f-f_0|}{f+f_0}\right]df\right]^{0.20} \tag{11}$$

where $R_{f_0}^{(1)}$ is the relative threshold elevation of a spatial frequency channel peaking at f_0 due to channel response $r_{f_0}^{(1)}$, and k_1 is a constant of proportionality to be determined empirically.

Equation (11) represents the predicted relation between the relative threshold elevation of a channel with peak sensitivity at f_0, and the spectral contrast function of the luminance distribution. When regarded as a function of f_0, the functionals of equation (11) will yield an envelope function which will be identified as the predicted relative threshold elevation function under Model 1.

Model 2. For Model 2, it will be assumed that the response of a spatial frequency channel, $r_{f_0}^{(2)}$, is proportional to the integral over frequency of the power spectrum of the stimulus weighted by a broad-band MTF:

$$r_{f_0}^{(2)} \propto \int_0^\infty \left[C(f)\exp\left(\frac{-4|f-f_0|}{f+f_0}\right)\right]^2 df. \tag{12}$$

Here the channel response will be proportional to the

[2] Below, a very weak dependence of threshold elevation upon channel response will be assumed. Therefore, slight deviations in predicted response due to slight variations in the form of the proposed MTF will be unimportant to the predicted threshold elevation.

[3] It is assumed that the spatial frequency channels do not distinguish between positive and negative frequencies, and thus all the spectral energy is assumed to be concentrated in the positive frequencies. This accounts for 0 as the lower limit of integration in equation (6).

[4] If $C(f)$ is complex, corresponding to an asymmetric stimulus distribution, the response is regarded as being proportional to the amplitude of the filtered spectral contrast function.

square of the nominal contrast of the sine-wave grating stimulus. Thus, with the aid of equations (9) and (12):

$$R_{f_0}^{(2)} = k_2(r_{f_0}^{(2)})^{0.10} = k_2\left\{\int_0^\infty \left[C(f)\exp\left(\frac{-4|f-f_0|}{f+f_0}\right)\right]^2 df\right\}^{0.10} \quad (13)$$

where $R_{f_0}^{(2)}$ is the predicted relative threshold elevation of the spatial frequency channel peaking at f_0, following adaptation to a stimulus with spectral contrast function $C(f)$. Considered as a function of f_0, equation (13) represents the predicted relative threshold elevation for Model 2.

Model 3. Model 3 assumes the existence of very narrow spatial frequency channels which respond in proportion to the amplitude of the spectral contrast function at the channel's nominal frequency.

$$r_{f_0}^{(3)} \propto C(f_0). \quad (14)$$

Since the amplitude of $C(f_0)$ is proportional to the nominal contrast for a sine-wave grating stimulus, equations (9) and (14) yield:

$$R_{f_0}^{(3)} = k_3(r_{f_0}^{(3)})^{0.20} = k_3[C(f_0)]^{0.20}. \quad (15)$$

Here, $R_{f_0}^{(3)}$ is the predicted relative threshold elevation following adaptation to a luminance distribution of spectral contrast $C(f_0)$ at frequency f_0.

A fourth model would assume that a spatial frequency channel has narrow-band sensitivity around some frequency f_0, and responds in proportion to the value of the contrast power spectrum at frequency f_0:

$$r_{f_0}^{(4)} \propto [C(f_0)]^2. \quad (16)$$

With the aid of equations (9) and (16)[5], it can be shown that the corresponding relative threshold elevation is identical with that predicted by Model 3, as given in equation (15).

Model 3 thus states that a spatial frequency channel at frequency f_0 will respond in proportion to the spectral contrast function or to the "energy density" at that frequency.

These three models represent the simplest quantitative formulations of a Fourier transform theory of suprathreshold visual processing. They contain only the necessary elements for such a theory—specification of the channel MTF, a channel stimulus/response characteristic, and a relation between the channel response and an observable variable. The candidate MTFs and stimulus/response functionals represented in the three models were chosen to be broadly representative of proposals found in the spatial frequency literature. The assumed power function relation between channel response and relative threshold elevation is conservative in that it leads to a lower bound on the predicted relative threshold elevation following adaptation to a stimulus distribution.

METHOD

Stimulus generation

Two kinds of luminance distributions were used as stimuli during the experiments—sine-wave modulation of a mean luminance level, and a bright, narrow bar superimposed on the same mean luminance level. In each case, the entire display subtended a square 1.75° on a side, at a distance of 286 cm from the observer. (Figure 1 illustrates the optical arrangements.) The display had a mean luminance of 4.63 cd/m^2, with a black surround. Subjects viewed the display monocularly through a 3 mm artificial pupil. In order to prevent the formation of after images and to vary the absolute phase of spectral components, they were instructed to move their points of fixation back and forth slowly across the display during periods of adaptation.

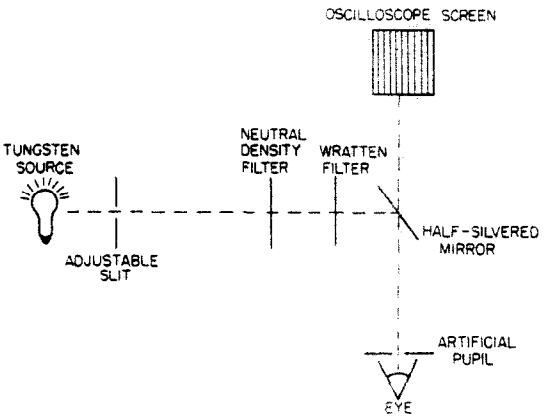

Fig. 1. Schematic diagram of the optics. Details in the text.

A field of uniform luminance was produced on the face of a Tektronix 502 oscilloscope, with a P2 bluish green phosphor, in the manner described by Campbell and Green (1965). The uniformity of the display was checked using a Pritchard Spectra Spot Photometer.

Sine-wave modulation. Stable, sine-wave modulation of the uniform luminance field was produced by applying sinusoidal voltages to the z-axis input of the oscilloscope, and triggering the display with the same signal. The transfer function of the oscilloscope (nominal contrast of the sinusoidal modulation as a function of z-axis frequency and voltage amplitude) was determined with a scanning slit and the Pritchard Spectra Spot photometer. During the experiments, all modulations were kept within the linear portion of this transfer function, corresponding to nominal contrasts of less than 0.30.

Spatial impulse. Formally, an impulse is a Dirac delta function. In practice, as an input to a system, it is an intense signal, sufficiently narrow (or brief), so that its fine structure cannot be resolved by the system. Its Fourier transform is roughly constant within a range of frequencies determined by the resolving power of the system.

The use of an impulse as an input to a system is important for at least two reasons. First, determining the impulse response of a system which possesses suprathreshold linearity is an important tool of linear systems analysis, since this response is the modulation transfer function of the system. Secondly, in the same sense that a sine-wave is the simplest of stimuli in the spectral domain, an impulse is the simplest of stimuli in the nonspectral domain—in the present case, the spatial domain.

For the visual system, a one-dimensional spatial impulse is a very narrow bar stimulus of high luminance. The Fourier transform of such a stimulus will be relatively flat within some spatial frequency range, as determined by the line spread function of the visual optics.

In the present experiment, the spatial impulse was produced by passing intense incandescent light through a narrow slit of adjustable width. The light was subsequently passed through an appropriate neutral density filter, and through a Kodak Wratten 65 colour filter which approximately matched the hue of the oscilloscope phosphor. With

[5] For a sine-wave grating, the response $r_{f_0}^{(4)}$ will be proportional to the square of the nominal contrast. Then, from equations (9) and (16)

$$R_{f_0}^{(4)} = k_4(r_{f_0}^{(4)})^{0.10} = k_4[C(f_0)^2]^{0.10} = k_4C(f_0)^{0.20} = k_4r_{f_0}^{(3)} = R_{f_0}^{(3)}.$$

the aid of a thin piece of flat glass, acting as a half-silvered mirror, the optical image of the impulse was superimposed on that of the oscilloscope screen (see Fig. 1). The impulse was placed at the same optical distance as the oscilloscope, and its long dimension, the vertical, subtended 1.75° of visual angle.

Except as specified for one of the control experiments, the luminance of the impulse as measured at the location of the observer's eye, was 140 cd/m^2. The luminance level was measured to be constant, within 12% over the length of the slit. The width of the slit was set to subtend 0.6′ of visual arc.

There are two main sources of slit image broadening in the optics prior to the retina. First, back surface reflections from the half-silvered mirror almost double the image width. Second, the optics of the visual system, even for emmetropic subjects, will impose a nonnegligible broadening of such a narrow image. Double passage ophthalmoscopic methods (Westheimer and Campbell, 1962; Krauskopf, 1962) have shown that for a focused eye and 3 mm artificial pupil, an upper bound for the line spread function is a half width of 1′ at half intensity. Investigations with laser interference fringes (Campbell and Green, 1965) and improved ophthalmoscopic methods (Campbell and Gubish, 1966) have shown that the line spread function is considerably narrower than this.

In view of these considerations, a retinal line spread function of 2′ has been assumed. This means that the energy in the ideal image of the illuminated slit is assumed to be distributed uniformly over a corresponding retinal image of 2′ width. In Fig. 2, curves labelled 0.6′, 1.0′, 2.0′ and 3.0′, represent Fourier transforms of retinal images broadened to the width indicated. Broadening the slit image leads to a decrease in the frequency range for which the transform of the image is roughly constant.

The assumption of a 2′ line spread function is regarded as an over estimate since each of the experimental subjects was able to detect peaks and valleys in sinusoidal modulation of more than 30 c/deg. At these frequencies, each cycle subtends less than 2′ of arc.

The slit appeared as a single, bright, narrow filament superimposed on the background field of the oscilloscope.

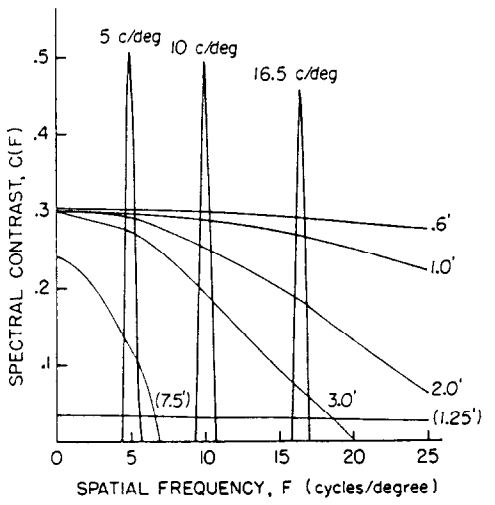

Fig. 2. Spectral contrast functions for experimental stimuli: those labelled 0.6′, 1.0′, 2.0′ and 3.0′ are the spectra of the spatial impulse (of objective width 0.6′, and luminance 140 cd/m^2) as broadened to the indicated widths by the optics. Spectra labelled (1.25′) and (7.5′) are for impulse stimuli of these widths but with luminance only twice the background luminance of 4.63 cd/m^2. Spectra labelled 5, 10 and 16.5 c/deg are those of the adapting sine-wave grating stimuli. In the latter, fine structure beyond the central bulge is not shown.

Table 1. Paradigm of the main experiment

Session No.	Condition
1–3	Training
4	Adaptation to 5 c/deg sine-wave grating of contrast 0.29
5	Adaptation to 9 c/deg sine-wave grating of contrast 0.26*
6	Adaptation to 16.5 c/deg sine-wave grating of contrast 0.20
7	Adaptation to vertical impulse of objective width 0.6 and luminance 140 cd/m^2
8	Adaptation to horizontal impulse of objective width 0.6′ and luminance 140 cd/m^2
9	Observation of nominal contrast threshold in the absence of pattern adaptation

* In this condition, subject JG was adapted to 10 c/deg, rather than 9 c/deg.

Experimental procedure

The experimental paradigm consisted of nine separate, 2–3 hr sessions, as listed in Table 1. The subjects' task was to adjust the nominal contrast of sinusoidal grating stimuli to the threshold of visibility (method of adjustment), by turning the knob of a potentiometer that controlled the sinusoidal voltage amplitude applied to the z-axis input of the oscilloscope.

The frequencies of the vertically oriented test gratings ranged from 2.2 to 20.0 c/deg. In each session, the nominal contrast threshold function was obtained over the entire range of frequencies.

The first three sessions were for training. Subjects learned to make contrast threshold settings from below, in less than 20 sec, and often less than 10 sec.

Sessions 4–8 contained the various adaptation conditions. Each of these sessions proceeded according to the following schedule:

(1) 15 min of brightness adaptation to the mean luminance level of 4.63 cd/m^2;

(2) a series of contrast threshold settings, two at each of the 14 test frequencies ranging from 2.2 to 20.0 c/deg: These initial unadapted threshold settings were subsequently used in the data analysis to establish the level of the subjects' contrast threshold function;

(3) a period of 15 min exposure to the adapting pattern for the session—e.g. in session 4, 15 min adaptation to a 5.0 c/deg sinusoidal grating of contrast 0.29; and

(4) a series of contrast threshold settings, 4 at each of the test frequencies. Between each of these settings, a period of 50–60 sec readaptation to the adapting pattern was given.

In (2) and (4) above, the test frequencies were presented in random order, with the constraint that adjacent frequencies never be presented sequentially.

In the ninth session, subjects made eight unadapted contrast threshold settings at each of the 14 test frequencies. These results were used to establish the subject's contrast threshold function.

Two control experiments required only sessions 1–4, 7, 9 and two separate conditions—adaptation to an impulse and adaptation to a 5.0 c/deg grating, each of half the standard amplitudes.

The nominal contrast of the adapting gratings in sessions 4–6 was chosen to be equal to the spectral contrast at corresponding frequencies for the vertical impulse of session 7, when optically broadened to a width of 2′.

Spectral contrast functions of the three adapting gratings are shown in Fig. 2, labelled as 5.0, 10.0 and 16.5 c/deg.

Subjects

Three subjects were used, two in the main experiment, and one in the control experiments. All three were students of college age, two females and one male, and each naive to the experimental hypotheses. All three subjects were emmetropic, with normal colour vision, according to their most recent ophthalmological examination. Each was given more than 6 hr of training and thus was highly practiced in the experimental task.

RESULTS

Method of analysis

The adaptation conditions were designed to measure the effects of various adapting stimuli upon the contrast threshold function of the observers. The relative threshold elevation $R(f)$, defined in equation (1), was the measure employed. This measure requires the use of both pre- and post-adaption data at each frequency. Because of time constraints, only a small sampling of pre-adaptation settings could be made. Accordingly, the following procedure was used for determining the unadapted contrast threshold function for any given session.

Session 9 was devoted to a determination of the unadapted contrast threshold function. The experimental points in Figs. 3(a) and (b) represent these functions for subjects TB and JG. In each case, these points were given a least-squares fit by a cubic polynomial function, the smooth curves shown in Figs. 3(a) and (b). This cubic function was then used as the unadapted contrast threshold function in the analysis of data from the adaptation conditions, sessions 4–8. Because the unadapted threshold function appeared to drift up and down slightly from session to session, the vertical position of the cubic polynomial approximation was shifted in accordance with a least squares fit to the unadapted threshold data collected at the beginning of each session. This method for establishing the unadapted threshold function worked well for all frequencies but the lowest, 2.2 and 3.0 c/deg. For these, the cubic polynomial approximation was found to be inadequate. For these frequencies, the two unadapted threshold settings, obtained for each frequency in each of the adaptation conditions, were used directly to establish the level of the unadapted threshold contrast.

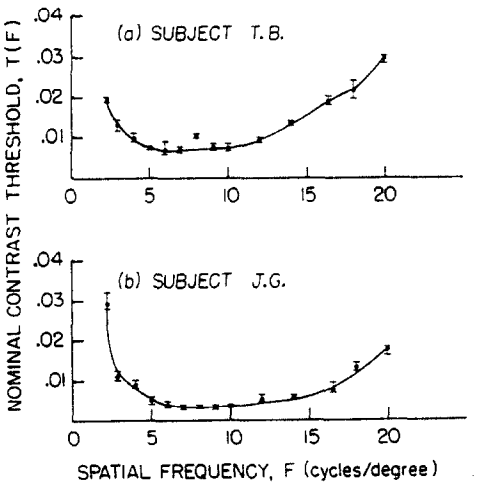

Fig. 3. (a) Subject TB: Nominal contrast threshold $T(f)$ as a function of spatial frequency f, under conditions of no pattern adaptation. The points are geometric means of eight settings. The error bars correspond to ± 1 S.E. of the log threshold values. The smooth curve is a least squares cubic polynomial fit to the points. (b) Same as in (a) for subject JG.

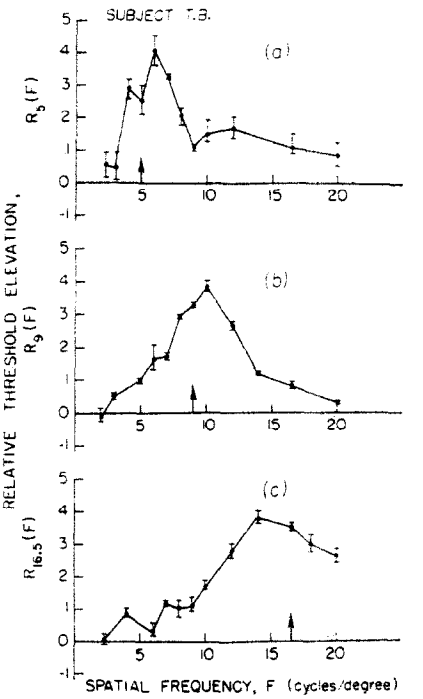

Fig. 4. Subject TB: (a) Relative threshold elevation $R_5(f)$ as a function of spatial frequency f, for adaptation to a sine-wave grating of nominal frequency 5.0 c/deg and nominal contrast 0.29. Relative threshold elevation is defined in equation (1). The points are geometric means of four settings. The error bars correspond to ± 1 S.E. of the difference in log contrast threshold before and after pattern adaptation. (b) $R_9(f)$ as a function of f for adaptation to a sine-wave grating of nominal frequency 9.0 c/deg and nominal contrast 0.26. (c) $R_{16.5}(f)$ as a function of f for adaptation to a sine-wave grating of nominal frequency 16.5 c/deg and nominal contrast 0.20.

In Figs. 4–7, values of the relative threshold elevation $R(f)$ are always geometric means of four values of the ratio $T_a(f)/T_b(f)$, minus 1. The measure of variability corresponds to ± 1 S.E. of the difference (log $T_a(f)$ − log $T_b(f)$).

The higher estimates of variability at 2.2 and 3.0 c/deg are reflections of the aforementioned method for treating the data for these two frequencies.

Adaptation to sine-wave gratings

Figures 4(a), (b) and (c) show the relative threshold elevation functions for subject TB's adaptation to sine-wave gratings of frequencies 5.0, 9.0 and 16.5 c/deg respectively.

In these plots, an ordinate value of 0 represents no effect of the adaptation. A negative value represents an increased sensitivity following adaptation. No particular significance is attached to the few negative values which do occur. It is assumed that they result from slight, intersession decreases in unadapted threshold, or from the variance of threshold settings.

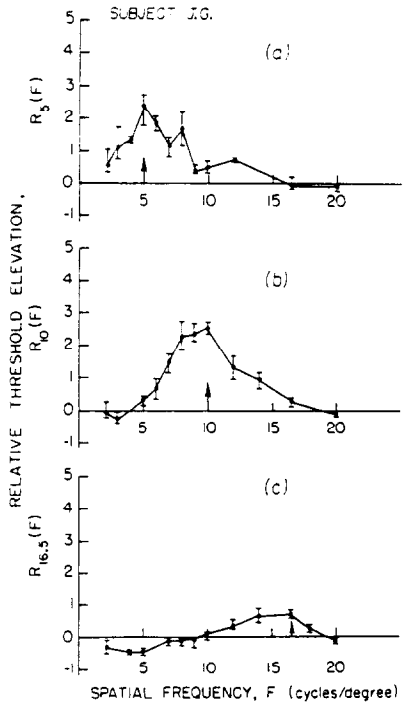

Fig. 5. Subject JG: same as for Fig. 4, except that Fig. 5(b) is for adaptation to a sine-wave grating of nominal frequency 10.0 c/deg and nominal contrast 0.25.

Figures 5(a), (b) and (c) show the corresponding data for subject JG.

Adaptation to the spatial impulse

In Figs. 6 and 7, the data points, spanned by their error bars, represent the relative threshold elevation following adaptation to the spatial impulse. Notice that this adaptation is very slight when compared to the adaptation obtained with the sine-wave gratings. Where they occur, significant deviations from an ordinate value of 0 are small. For the two subjects, the maximum value of relative threshold elevation following adaptation to the impulse was 0.80, whereas peaks of the relative threshold elevation functions following grating adaptation ranged from 0.70 to 4.03.

Analogous data, not shown[6], were obtained for the spatial impulse in horizontal orientation. The effects of this adaptation were even less than for the vertical impulse.

TESTS OF THE THREE FOURIER TRANSFORM ADAPTATION MODELS

Equations (11), (13) and (15) represent explicit models which predict the relative threshold elevation following adaptation to arbitrary luminance distributions. These equations contain the constants of proportionality k_1, k_2 and k_3, which are determined empirically, using the data from the sine-wave grating adaptation conditions.

[6] Since adaptation to a horizontal impulse would not be predicted to affect the contrast threshold for vertical sine-wave gratings, these results are not of theoretical relevance to the present discussion.

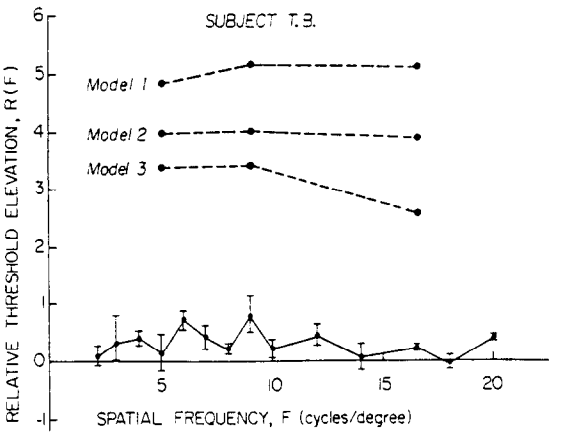

Fig. 6. Subject TB: the data points, connected by straight line segments, represent the experimentally determined relative threshold elevation $R(f)$ as a function of spatial frequency f, following adaptation to a spatial impulse of objective width 0.6', luminance 140 cd/m^2, superimposed on a background luminance of 4.63 cd/m^2. The points are geometric means of four settings. The error bars correspond to ± 1 S.E. of the difference in log contrast threshold before and after pattern adaptation. The points, connected by dashed lines, at 5.0, 9.0 and 16.5 c/deg are the predicted values of the three Fourier transform models for the relative threshold elevation following adaptation to the spatial impulse. The dashed lines represent interpolations between these points. The values predicted by Model 1 are derived from equation (11) which represent a system of broad-band channels with response proportional to the filtered contrast spectrum of a stimulus. The values predicted by Model 2 are derived from equation (13) which represents a system of broad-band channels with response proportional to the filtered contrast "power" spectrum of a stimulus. The values predicted by Model 3 are derived from equation (15) which represents a system of narrow-band channels with response proportional to either the contrast spectrum or "power" spectrum of a stimulus.

To do so, the spectral contrast function $C(f)$ must be specified for the adapting sinusoidal luminance distribution. For an adapting sine-wave grating of amplitude a, nominal frequency f_0, spatial width w, superimposed upon a mean luminance L_0, $C(f)$ is given by:

$$C(f) = \frac{wa}{L_0} \cdot \frac{\sin[\pi w(f - f_0)]}{\pi w(f - f_0)}. \qquad (17)$$

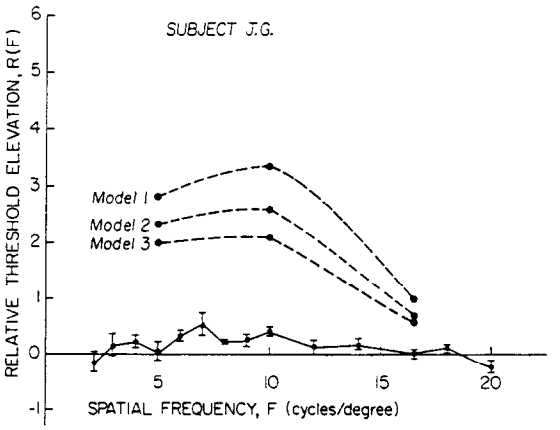

Fig. 7. Subject JG: same as for Fig. 6.

Table 2. Relative threshold elevation constants

Spatial frequency	Relative threshold elevation constants		
f	k_1	k_2	k_3
	Subject JG		
5.0	2.57	2.55	2.37
10.0	2.79	2.77	2.58
16.5	0.79	0.77	0.73
	Subject TB		
5.0	4.42	4.39	4.08
9.0	4.28	4.25	3.96
16.5	4.27	4.25	3.95

Given $C(f)$, and the corresponding peaks of the relative threshold elevation functions, obtained from Figs. 4 and 5, the constants k_1, k_2 and k_3, can be solved for [7]. Table 2 lists the constants at each of the three adapting frequencies for subjects TB and JG. Because they vary, not only between subjects, but between frequencies for the same subject, the adaptation characteristics of individual spatial frequency channels vary. These variations will mean that the three Fourier transform models are calibrated only for the specific spatial frequencies for which sine-wave grating adaptation was measured.

Finally, the three Fourier transform models can be tested by comparing their predictions with the empirical results already presented.

The hypothetical relative threshold elevation functions following adaptation to a spatial impulse will be specified with the use of equations (11), (13) and (15), and with the use of the constants in Table 2. The spectral contrast function for the adapting 2′ impulse is given by:

$$C(f) = (0.30)\frac{\sin(0.033\,\pi f)}{0.033\,\pi f}. \qquad (18)$$

This function is shown as the curve labelled 2.0′ in Fig. 2.

The relative threshold elevation functions predicted by the three models, as a consequence of adaptation to a spatial impulse, are shown in Figs. 6 and 7 for subjects TB and JG respectively. In both cases, the relative threshold elevations at each of the three calibrated frequencies is plotted for each of the three models. The dashed lines represent interpolations between the predicted values.

Compare the three hypothetical relative threshold elevation functions with the empirical results for adaptation to the spatial impulse, as shown in Figs. 6 and 7. At every point, the hypothetical functions lie well above the error bars of the empirical data. It is clear, then, that granting the assumptions of the experimental method, these three models are falsified by the empirical results. They may, accordingly, be rejected as completely adequate.

Recall that these three models are of a minimum character, i.e. they contain only the elements necessary to a quantitative formulation. Furthermore, the specifications of the three models have been chosen to bracket most of the channel response functionals proposed in the spatial frequency literature. Finally, all assumptions made in the theoretical computations and in the methods of analysis are regarded as conservative, i.e. tending to favour the adequacy of the Fourier transform models. As applied to the analysis of narrow, luminous bars, then, this broad subset of Fourier transform models appears to be inadequate. Compared with the predictions of the models, there is virtually no adaptation to the spatial impulse.

CONTROL EXPERIMENTS

Two factors that might complicate the foregoing results were considered in two control experiments with a third subject. Ultimately, neither factor affected the foregoing conclusions.

Receptor nonlinearity

There is electrophysiological evidence (Normann and Werblin, 1974; Boynton and Whitten, 1970) that vertebrate photoreceptors respond linearly only over a limited luminance range with respect to some mean adapting luminance. For instance, the primate cone response (Boynton and Whitten, 1970) is linear for test luminances only 1–2 log units above or below the adapting background luminance.

In the present experiment, the adapting spatial impulse, of width 0.6′, had an objective luminance of 140 cd/m^2, a factor of 30 greater than the background luminance of 4.63 cd/m^2, upon which it was superimposed. The possibility thus exists that human photoreceptors respond nonlinearly to intensities ranging a factor of 30 above 4.63 cd/m^2. Of course, if the retinal image of the impulse has been broadened to a width of 2′ by the system optics, as assumed, then the effective luminance will have been reduced to $140 \times 0.6/2 = 42$ cd/m^2. A luminance of 42 cd/m^2 represents less than one log unit difference from the background luminance of 4.63 cd/m^2, and would be expected to lie within the linear range of human photoreceptors.

However, as a partial check for the possibility of photoreceptor nonlinear response, a third subject, JK, was adapted with a spatial impulse of objective luminance 70 cd/m^2. In other respects, this control experiment was identical to the main experiment, except that calibration data were taken only at 5.0 c/deg and with an adapting contrast of 0.14. Accordingly, predictions of the three models are computed only for a frequency of 5.0 c/deg.

In Table 3, the first two rows give the predictions of the three Fourier transform models for the relative threshold elevations following adaptation to spatial impulses of 140 and 70 cd/m^2. For each, the final two columns give the geometric mean of four data points, with the corresponding measure of variability (previously discussed). The hypothetical values are again too high in all cases.

The conclusion to be drawn from this control experiment is that photoreceptor nonlinearity does not account for the lack of adaptation to the spatial impulse.

Power function transformation of the stimulus distribution

Stevens (1957) and others have shown that the perceived brightness of a test target is related to the luminance of the test target by a power function relation. In the dark adapted eye, the exponent of the brightness function

[7] For Models 1 and 2, this computation will require carrying through the integrations on the right of equations (11) and (13). To facilitate these two integrations, the following two simplifying approximations were made: (1) the effective portion of the spectral contrast function for the adapting sine-wave gratings lies between its central two zeros, $f_0 \pm 0.57°$. (2) Within the region $f_0 \pm 0.57°$, the channel MTF is assumed to be constant and equal to 1.0.

Table 3. Data from the control experiments with subject JK

Condition	Predictions of Model 1	Model 2	Model 3	Observed Relative threshold elevation at 5.0 c/deg:	Error bar
Impulse of 140 cd/m^2	1.05	0.90	0.74	0.15	0.04–1.28
Impulse of 70 cd/m^2	0.92	0.79	0.65	0.05	−0.06–0.18
Power function transformed impulse of 140 cd/m^2	0.76	0.63	0.60	0.15	0.04–0.28

remains constant at 0.33, except for very brief or very small targets (Mansfield, 1973). However, light adaptation produces a steepening of the brightness function both following an adapting stimulus (Stevens and Stevens, 1963), or when the target is superimposed on the adapting background (Onley, 1961). Stevens and Stevens (1963) obtained the following power function relation between brightness B and luminance L for light-adaptation to a luminance on the order of 4 cd/m^2:

$$B = 3.6(L - 0.027)^{0.355} \quad (19)$$

where B is the brightness in brils, L is the luminance in cd/m^2, 0.027 is a threshold value, and the exponent 0.355 holds only for light-adaptation to a luminance of the order 4 cd/m^2. Their results were derived from brightness estimates of 2 sec test flashes subtending 5.7° superimposed upon adapting background fields subtending 58°. They found that the power function exponent increased from 0.33 to 0.44 as the adapting luminance varied from 0 to 3400 cd/m^2. The value of 0.355 is in accordance with the luminance of the background fields of 4.63 cd/m^2 used in the current experiments.[8]

The possibility arises that the computations of the three models are not done upon the spectral contrast function $C(f)$, but upon a corresponding function derived from the stimulus distribution followed by a power function transformation. It may be that the Fourier adaptation models apply in the brightness domain rather than in the luminance domain.

A second control experiment was performed with subject JK. Here, all computations with the stimulus distribution were done following the power function transformation of equation (19)[9]. The standard impulse of 140 cd/m^2 was used as the adapting stimulus. However, calibration data was obtained from adaptation to a 5.0 c/deg sine-wave grating of nominal contrast 0.14.

In Table 3, the third row gives the relative threshold elevation predictions at 5.0 c/deg, for the three Fourier transform adaptation models in the brightness domain. The final two columns give the empirical results.

It is apparent that even when computations are done in the brightness domain, the hypothetical predictions of the three Fourier transform adaptation models greatly exceed the empirical values for the relative threshold elevation.

The conclusion to be drawn from the second control experiment is that the lack of adaptation to the spatial impulse cannot be accounted for, in the context of the Fourier transform models, by a power function transformation of the stimulus.

DISCUSSION

Campbell, Carpenter and Levinson (1969) examined the threshold for visibility of aperiodic patterns derived from sine-wave gratings—single half-cycle or "bar", single full-cycle sinusoid, and edge between a sine-wave grating and a uniform field. Their work with aperiodic stimuli corresponds in kind to the work of Campbell and Robson (1968) with periodic stimuli. As with the latter, Campbell *et al.* (1969) found success in predicting the contrast threshold of the aperiodic stimuli from their spectral content. These results do not conflict with those of the present paper, since they represent evidence only for small signal linearity. The present experiments, like those of Blakemore and Campbell (1969), are concerned with the response of the visual system to suprathreshold stimuli.

A complicating possibility, suggested by Campbell *et al.* (1969) is that the pattern threshold criterion might change with the form of the stimulus being detected. For example, a single bar might be detected by a peak-to-through detector, while a sine-wave pattern of a number of cycles might be detected by means of some spectral parameter. The present experiments are free of this complication since all the data are derived from threshold settings for sinusoidal gratings. To the extent that the threshold mechanism remains constant for a given stimulus type, constancy of mechanism can be assumed throughout these experiments.

[8] Stevens and Stevens (1963) used large adapting fields and a natural pupil. These conditions yield higher values of retinal illuminance for a given mean luminance than the conditions of the present study. Accordingly, an estimate of 0.355 for the brightness exponent may be slightly high for use in the present work. However, any appropriate downward correction will have negligible effect upon the theoretical predictions of Table 3.

[9] When a target source is placed in proximity to a brighter "glare" source, the perceived brightness of the target is decreased, but the exponent of its brightness power function is increased (Stevens, 1966). These effects are not relevant to the power function transformation of the spatial impulse because it is much brighter than the uniform background, but the point-by-point transformations of the sine-wave distributions may be affected because they vary both above and below the mean luminance. The latter possibility is consonant with the finding that perceived contrast varies as a power function of nominal contrast with comparatively high exponents (Franzen and Berkley, 1975). Despite this possible complication, equation (19) is used for the present computations because they are meant to demonstrate that even an extreme response compression, such as that represented by the relation between brightness and luminance, will not affect the general conclusions of this paper.

In two of their experiments, Sullivan, Georgeson and Oatley (1972) attempted to assess the effects on the relative threshold elevation function of adaptation to bars of width 7.5′ and 1.25′. They have reported slight adaptation to these stimuli, not unlike that shown here in Figs. 6 and 7, and not exceeding relative threshold elevations of 0.8. Unfortunately, the luminance of their adapting bars was so low that the corresponding spectral functions would not be expected to produce substantial adaptation. They used bars whose peak intensity was less than twice the background intensity. In Fig. 2, spectral functions for bars of 1.25′ and 7.5′ width, and peak intensity twice the mean intensity of 4.63 cd/m^2, are shown. These functions are labeled (1.25′) and (7.5′). Both of these functions lie well below the spectral function for the adapting impulse used in the present experiments.

Weisstein and Bisaha (1972) used a forward masking paradigm. They examined the effect of masking with square-wave gratings or single dark bars upon magnitude estimates of the contrast of subsequently presented like stimuli. The bars were dark half-cycles of square-waves, and had widths of 2′, 3′ and 10′. The spectral contrast functions of these bars are similar to those of Sullivan *et al.* (1972), and thus would not be expected to have strong adapting or masking effects, according to the Fourier transform models of this paper. Thus, the observation of Weisstein and Bisaha that a dark bar masks a grating uniformly over the grating field, is hard to interpret in the context of the Fourier models.

The preceding analysis and experiments argue that quantitative Fourier transform models for the processing of suprathreshold visual patterns make predictions of the corresponding visual response which are not confirmed. These models predict strong spatial frequency adaptation following exposure to a spatial impulse contained within a foveal field of 1.75° by 1.75°. Despite the spectral richness of the impulse, however, only slight adaptation was observed. These results suggest that, for visual fields of 2° dia, or more, modulation transfer function approach cannot be applied in a simple way, to the visual processing of aperiodic stimuli.

It may be possible to interpret the lack of spatial frequency adaptation to the spatial impulse as an extreme case of what Tolhurst (1972) and Dealy and Tolhurst (1974) term "inhibition between spatial frequency channels". Tolhurst (1972) found that the relative threshold elevation produced by adaptation to a square-wave was less than the summed effects of its constituent first and third harmonics, presented independently. He hypothesized that, at suprathreshold levels of response, spatial frequency channels exert mutual inhibition upon each other. For the case of the impulse, Fourier models would predict that all low frequency channels should respond vigorously, hence, perhaps, generating a great deal of mutual inhibition. This inhibition of response might account for the subsequent lack of adaptation. Although this explanation of the present results must be considered rather unlikely, its acceptance would not save the Fourier model since it would entail a breakdown in the presumed independence between spatial frequency channels.

Phase detection

An explanation for the present results may be found in a model of phase detection in vision. Relative phase may be unimportant to the threshold detection of complex gratings consisting of two spatial frequency components (Graham and Nachmias, 1971; Nachmias and Weber, 1975; Barfield and Tolhurst, 1975), although Stromeyer and Klein (1974) have demonstrated a small relative phase dependence. However, phase-specific perceptual effects do occur upon exposure to suprathreshold gratings of this kind (Stromeyer, Lange and Ganz, 1973; Atkinson and Campbell, 1973). The fact that people can localize objects in visual space argues for the existence of a phase detection mechanism.[10]

In the present experiments, subjects were instructed to move their points of fixation back and forth across the display. Accordingly, the absolute phase of the spectral components of all stimuli were continuously varied, but retained a constant relative phase. For the sine-wave gratings, all spectral components were in phase with respect to the central luminance peak, while for the impulse, all components were in phase with respect to an origin defined by the location of the center of the bar.

Receptive field model and phase-encoding. As used in linear optics, the modulation transfer function is a real quantity defined in terms of the Fourier transform of a line spread function (Linfoot, 1964). For a d.c. independent, linear system with space-invariant line spread function $W(x)$, the transmitted image $I(x)$ resulting from a stimulus distribution $L(x) = L_0 + a\cos(2\pi fx + \delta)$ is:

$$I(x) = a\mathrm{MTF}(f)\cos(2\pi fx + \delta + \phi(f)) \qquad (20)$$

$\mathrm{MTF}(f)$ is defined to be the modulation transfer function and is the magnitude of the Fourier transform of $W(x)$. $\phi(f)$ is a phase-shift function and is the complex phase of the Fourier transform of $W(x)$. It is nonzero when the line spread function is asymmetrical. Both the MTF and phase-shift functions depend only on the frequency f of the stimulus distribution, and are independent of its phase δ. The phase-independence property of the MTF is a consequence of the assumed space-invariance of the line spread function $W(x)$ (Linfoot, 1964; Bracewell, 1965). Without this assumption, the MTF is undefined.

Models based on the MTF, like those discussed in this paper, assume a system or channel response dependent upon the stimulus amplitude spectrum weighted by the MTF. Since both these functions are phase-independent, so too is the response related to them.

The lack of phase sensitivity and the assumed space-invariant line spread functions of the MTF formulation both contradict receptive field models based on electrophysiological results. An alternative to the global MTF approach for the modelling of spatial frequency phenomena has been suggested by Macleod and Rosenfeld (1974). Instead of discussing spatial frequency channels independent of their spatial proper-

[10] The amplitude function of the Fourier transform is invariant under spatial translation, but the phase function is not.

ties, they have suggested that pattern detection may be modelled by an ensemble of centre–surround receptive fields, varying in response profile and position in visual coordinates. A linear receptive field model assumes point-by-point convolution of the stimulus luminance distribution with a receptive field response profile. The receptive fields will, in general, differ in shape from point to point and, in the simplest case, be independent. If each is regarded as a separate channel, it is no longer appropriate to assume a space-invariant line spread function and the modulation transfer function is no longer defined.

For a receptive field channel located at position x_0 with response profile $W_{x_0}(x - x_0)$, the response to an arbitrary luminance distribution $L(x)$ is given by:

$$R_{x_0} = \int_{-\infty}^{\infty} L(x) W_{x_0}(x - x_0)\,dx. \qquad (21)$$

For a d.c. independent unit, the response to a sinusoidal luminance distribution of the form given above is:

$$R_{x_0} = aM_{x_0}(f)\cos[2\pi f x_0 + \delta + \phi_{x_0}(f)] \qquad (22)$$

where $M_{x_0}(f)$ and $\phi_{x_0}(f)$ are the magnitude and phase functions, respectively, of the Fourier transform of the response profile. Consider the differences between equations (20) and (22). In the former, x is a continuous variable and the system response is later defined to be related only to the factor $a\mathrm{MTF}(f)$. In the latter, x_0 identifies the spatial location of a channel, and its response is represented by the entire right side of equation (22). The response of the receptive field channel thus depends not only on the frequency f of the stimulus distribution, but also on its phase δ. This dependence represents the fact that some receptive fields are optimally aligned with the stimulus, while others are out of phase with it.

The MTF approach may be translated into the language of linear receptive fields by assuming that all receptive fields of a given response profile type feed into a single "channel" whose frequency selectivity is determined by the frequency response of the individual inputs. In this case, the position x_0 in equation (22) can be regarded as a continuous variable and the response of the "channel" is dependent upon the factor $aM_{x_0}(f)$. Although Hubel and Wiesel (1965) have postulated the hierarchical convergence of similar units in the visual cortex to yield higher order receptive fields, there is little evidence for the kind of global, space-invariant receptive fields required by the MTF approach.

In this connection, the physiological models of piecewise Fourier decomposition in the visual cortex (Pollen and Taylor, 1974; Pollen and Ronner, 1975; Glezer, Ivanoff and Tscherbach, 1973) have been examined by Robson (1975), and found to be of only limited, qualitative utility.

The receptive field model is most easily treated in the space-domain. Here, collaborative effort between cells such as probability integration (King-Smith and Kulikowski, 1975), or response integration (Stromeyer and Klein, 1975) may be explicitly postulated and tested. The MTF appraoch is most appropriate to a frequency-domain analysis in the case of linear, space-invariant systems. The results of the experiments reported in this paper, together with electrophysiological data suggest that this is not the case with the human visual system.

A quantitative formulation of the receptive field model requires the specification of a number of parameters for the description of the receptive fields. These include characterization of the response profiles in terms of the number and width of excitatory and inhibitory zones, the position and orientation of receptive fields, and the distribution of receptive field types. Such a formulation must also specify how the ensemble of receptive fields participate in the determination of psychophysical thresholds. Work in progress by the author indicates that many spatial frequency phenomena can be accounted for by such a quantitative formulation.

Qualitatively, the receptive field model easily accounts for the lack of adaptation to the spatial impulse. According to it, a relatively small number of pattern detecting receptive fields are stimulated, and adapted, by the narrow luminous bar. The unadapted majority are left to detect the test sine-wave gratings. If eye movements are considered, none of the receptive fields are stimulated for more than a small portion of the total exposure time, but perhaps enough to produce the slight adaptation actually observed. In contrast, under full field adaptation to periodic stimuli, all of the hypothetical foveal receptive fields would be exposed for the entire adapting duration.

Acknowledgements—I am particularly indebted to Dr. R. J. W. Mansfield for his considerable advice, and many detailed comments and criticisms. Thanks are also due to Dr. David M. Green, Dr. Y. Y. Zeevi and Dr. Richard Kronauer for their helpful comments and suggestions concerning this work. I wish to thank Philip Turner for his aid in the preparation of the equipment and Wendy Willson Legge for her help in many phases of the work. The support of the Canada Council and of the National Research Council of Canada are gratefully acknowledged.

REFERENCES

Atkinson J. and Campbell F. W. (1974) The effect of phase on the perception of compound gratings. *Vision Res.* **14**, 159–162.

Barfield L. and Tolhurst D. J. (1975) The detection of complex gratings by the human visual system. *J. Physiol., Lond.* **248**, 37P–38P.

Blakemore C. and Campbell F. W. (1969) On the existence of neurones in the human visual system selectivity sensitive to the orientation and size of retinal images. *J. Physiol., Lond.* **203**, 237–260.

Blakemore C. and Sutton P. (1969) Size adaptation: a new aftereffect. *Science, N.Y.* **166**, 245–247.

Boynton R. M. and Whitten D. (1970) Visual adaptation in monkey cones: recordings of late receptor potentials. *Science, N.Y.* **170**, 1423–1426.

Bracewell R. (1965) *The Fourier Transform and Its Applications*. McGraw-Hill, New York.

Campbell F. W. (1974) The transmission of spatial information through the visual system. In *The Neurosciences Third Study Program* (Edited by Schmitt F. O. and Worden F. G.), pp. 95–103. MIT, Cambridge, Mass.

Campbell F. W., Carpenter R. H. S. and Levinson J. Z. (1969) Visibility of aperiodic patterns compared with that of sinusoidal gratings. *J. Physiol., Lond.* **204**, 283–298.

Campbell F. W. and Green D. G. (1965) Optical and retinal factors affecting visual resolution. *J. Physiol., Lond.* **181**, 576–593.

Campbell F. W. and Gubisch R. W. (1966) Optical quality of the human eye. *J. Physiol., Lond.* **186**, 558–578.

Campbell F. W. and Robson J. G. (1968) Application of Fourier analysis to the visibility of gratings. *J. Physiol., Lond.* **197**, 551–566.

Dealy R. S. and Tolhurst D. J. (1974) Is spatial frequency adaptation an aftereffect of prolonged inhibition? *J. Physiol., Lond.* **241**, 261–270.

Franzen O. and Berkley M. (1975) Apparent contrast as a function of modulation depth and spatial frequency: a comparison between perceptual and electrophysiological measures. *Vision Res.* **15**, 655–660.

Glezer V. D., Ivanoff V. A. and Tscherbach T. A. (1973) Investigation of complex and hypercomplex receptive fields of the cat as spatial frequency filters. *Vision Res.* **13**, 1875–1904.

Graham N. and Nachmias J. (1971) Detection of grating patterns containing two spatial frequencies: a comparison of single-channel and multiple-channel models. *Vision Res.* **11**, 251–259.

Hoekstra J., van der Goot D. P. J., van den Brink G. and Bilsen F. A. (1974) The influence of the number of cycles upon the visual contrast threshold for spatial sine-wave patterns. *Vision Res.* **14**, 365–368.

Hubel D. H. and Wiesel T. N. (1965) Receptive fields and functional architecture in two non-striate visual areas (18 and 19) of the cat. *J. Neurophysiol.* **28**, 229–289.

King-Smith P. E. and Kulikowski J. J. (1975) The detection of gratings by independent activation of line detectors. *J. Physiol., Lond.* **247**, 237–271.

Krauskopf J. (1962) Light distribution in human retinal images. *J. opt. Soc. Am.* 52, 1046–1050.

Linfoot E. H. (1964) *Fourier Methods in Optical Image Evaluation.* Focal, New York.

Macleod I. D. G. and Rosenfeld A. (1974) The visibility of gratings: spatial frequency channels or bar detecting units? *Vision Res.* **14**, 909–915.

Mansfield R. J. W. (1973) Brightness function: effect of area and duration. *J. opt. Soc. Am.* **61**, 913–920.

Nachmias J. and Weber A. (1975) Discrimination of simple and complex gratings. *Vision Res.* **15**, 217–225.

Normann R. A. and Werblin F. S. (1974) Control of retinal sensitivity. I: light and dark adaptation of vertebrate rods and cones. *J. gen. Physiol.* **63**, 37–61.

Onley J. W. (1961) Light adaptation and the brightness of brief foveal stimuli. *J. opt. Soc. Am.* **51**, 667–673.

Pantle A. and Sekuler R. (1968) Size detecting mechanisms in human vision. *Science, N.Y.* **162**, 1146–1148.

Pollen D. and Ronner S. (1975) Periodic excitability changes across receptive fields of complex cells in striate and parastriate cortex of the cat. *J. Physiol., Lond.* **245**, 667–697.

Pollen D. and Taylor J. (1974) The striate cortex and the spatial analysis of visual space. In *The Neurosciences Third Study Program* (Edited by Schmitt F. O. and Worden F. G.), pp. 239–247. MIT, Cambridge, Mass.

Quick R. F. and Reichert T. (1975) Spatial frequency selectivity in contrast detection. *Vision Res.* **15**, 637–643.

Robson J. G. (1975) Receptive fields: neural representation of the spatial and intensive attributes of the visual image. In *Handbook of Perception*, Vol. V: *Seeing* (Edited by Carterette E. C. and Friedman M. P.), pp. 81–116. Academic Press, New York.

Sachs M. B., Nachmias J. and Robson J. G. (1971) Spatial frequency channels in human vision. *J. opt. Soc. Am.* **61**, 1176–1186.

Savoy R. L. and McCann J. J. (1975) Visibility of low-spatial-frequency sine-wave targets: dependence on number of cycles. *J. opt. Soc. Am.* **65**, 343–350.

Stevens J. C. and Stevens S. S. (1963) Brightness function: effects of adaptation. *J. opt. Soc. Am.* **53**, 375–385.

Stevens S. S. (1957) On the psychophysical law. *Psychol. Rev.* **64**, 153–181.

Stevens S. S. (1966) Power-group transformations under glare, masking, and recruitment. *J. acoust. Soc. Am.* **39**, 725–735.

Stromeyer C. F. III and Julesz B. (1972) Spatial frequency masking in vision: critical bands and spread of masking. *J. opt. Soc. Am.* **62**, 1221–1232.

Stromeyer C. F. III and Klein S. (1974) Spatial frequency channels in human vision as asymmetric (edge) mechanisms. *Vision Res.* **14**, 1409–1420.

Stromeyer C. F. III and Klein S. (1975) Evidence against narrow-band spatial frequency channels in human vision: the detectability of frequency modulated gratings. *Vision Res.* **15**, 899–910.

Stromeyer C. F. III, Lange A. F. and Ganz L. (1973) Spatial frequency phase effects in human vision. *Vision Res.* **13**, 2345–2360.

Sullivan G. D., Georgeson M. A. and Oatley K. (1972) Channels for spatial frequency selection and the detection of single bars by the human visual system. *Vision Res.* **12**, 383–394.

Tolhurst D. J. (1972) Adaptation to square-wave gratings: inhibition between spatial frequency channels in the human visual system. *J. Physiol., Lond.* **226**, 231–248.

Weisstein N. and Bisaha J. (1972) Gratings mask bars and bars mask gratings: visual frequency response to aperiodic stimuli. *Science, N.Y.* **174**, 1047–1049.

Westheimer G. and Campbell F. W. (1962) Light distribution in the image formed by the living human eye. *J. opt. Soc. Am.* **52**, 1040–1045.